JOURNAL OF PROPULSION AND POWER
Vol. 11, No. 3, May–June 1995

Rocket Engine Coaxial Injector Liquid/Gas Interface Flow Phenomena

Wolfgang Mayer* and Gerd Krülle†
DLR, German Aerospace Research Establishment, Hardthausen 74239, Germany

Coaxial injectors are used for the injection and mixing of propellants H_2/O_2 in cryogenic rocket engines. The aim of the theoretical and experimental investigations presented here is to elucidate some of the physical processes in coaxial injector flow with respect to their significance for atomization and mixing. Experiments with the simulation fluids H_2O and air were performed under ambient conditions and at elevated counter pressures up to 20 bar. This article reports on phenomenological studies of spray generation under a broad variation of parameters using nanolight photography and high-speed cinematography (up to 3×10^4 frames/s). Detailed theoretical and experimental studies of the surface evolution of turbulent jets were performed. Proof was obtained of the impact of internal fluid jet motions on surface deformation. The $m = 1$ nonaxisymmetric instability of the liquid jet seems to be superimposed onto the small-scale atomization process. A model is presented that calculates droplet atomization quantities as frequency, droplet diameter, and liquid core shape. The overall procedure for implementing this model as a global spray model is also described and an example calculation is presented.

Introduction

THE injection and mixing of the propellants in cryogenic H_2/O_2 rocket engines is performed using coaxial injectors, where the liquid oxidizer jet ($u_l \sim 20$ m/s) is atomized by a surrounding fast gaseous fuel stream ($u_g \sim 250$ m/s). These atomization and flow phenomena define the physical boundary conditions for the following combustion process and are, therefore, most important preconditions for the ignition behavior and reaction stability of the rocket engine.

One of the major aims of the experimental and theoretical studies presented here is the creation of theoretical injection and atomization models, which in connection with combustion or other engine system component models, finally supports the improvement of existing and development of future rocket engines. These efforts have to be viewed in light of the general trend to support and possibly replace costly actual engine tests with numerical simulations. Theoretical work in this region has been done by Liang et al.[1] and Przekwas et al.[2] This article describes some of the recent results of the theoretical and experimental studies concerning coaxial atomization based on experiences of previous investigations that were summarized in Krülle et al.,[3] Farago,[4] and Buschulte.[5]

It is assumed here that atomization processes are to a large extent independent of the high temperatures found in real engines. This seems reasonable as indicated in H_2O_2 ignition experiments in a model combustion chamber using liquid oxygen and gaseous hydrogen. Therefore, coaxial atomization is treated here as a coldflow phenomenon.

Such coaxial atomization may be divided into five unique physical regimes. These are (main phenomena in parentheses, numbers refer to Fig. 1): 1) turbulent liquid core (liquid surface preshaping); 2) liquid/gas interface (primary atomization); 3) thick spray (secondary atomization, droplet breakup); 4) thin spray (turbulent droplet dispersion); and 5) gas flow region (operational conditions).

The atomization starts with liquid turbulence that results in a wavy jet surface. These surface waves grow or shrink under the action of aerodynamic and surface tension forces, respectively. Thereafter, a ligament or droplet is separated from this surface (primary breakup), which under certain conditions disintegrates once again (secondary breakup). The resulting droplets disperse under the influence of turbulence in the gaseous environment, which represents the main process of liquid/gas mixing. The latter is treated in detail in Mayer et al.[6]

Experimental Part

The physical complexity of coaxial atomization necessitates a cautious and well-informed conceptual approach in approximating the real engine condition.

The experimental research was done with the simulation fluids H_2O and air under both ambient and elevated pressure conditions.

Coaxial atomization is mainly controlled by the following parameters (see Fig. 2): diameter of inner tube d_i, gas gap width y, gas and liquid velocity $u_{g,l}$, density $\rho_{g,l}$, viscosity $\mu_{g,l}$, and surface tension σ_l. With these nine parameters it is possible to define a set of six nondimensional numbers containing y/d_i, u_g/u_l, ρ_g/ρ_l, μ_g/μ_l, Re_l, (Re_g), We_g, namely, the geometry, velocity, density and viscosity ratios, the liquid and gas Reynolds numbers, and the Weber number; the latter defined by

$$Re_l = \left(\frac{d_i \rho_l u_l}{\mu_l}\right) \tag{1}$$

$$Re_g = \left(\frac{y \rho_g u_g}{\mu_g}\right) \tag{2}$$

$$We_g = \left(\frac{d_i \rho_g u_g^2}{\sigma_l}\right) \tag{3}$$

where Re_g is redundant. Regarding these parameters, it is possible to define simulation experiments using model injectors and simulation fluids that are physically similar to applied rocket engine injection and atomization conditions. Table 1

Presented as Paper 92-3389 at the AIAA/SAE/ASME/ASEE 28th Joint Propulsion Conference and Exhibit, Nashville, TN, July 6–8, 1992; received March 16, 1993; revision received April 19, 1994; accepted for publication May 31, 1994.

*Research Engineer, Injection Research Group. Member AIAA.
†Associate Professor, Head System Analysis and Injection Research. Member AIAA.

Table 1 Characteristic parameters of coaxial atomization, comparison between typical GH_2/LO_2 coaxial injectors with model injectors using H_2O/air as fluids

	Fluids						
	LO_2/GH_2				H_2O/air		
					Model		
Injector type	SSME, Preb[a]	SSME, Ch[b]	HM60, Ch	HM7, Ch	I	II	Typical values
y/d_i	0.3	0.4	0.1	0.3	0.4	1.3	0.3
u_g/u_l	11.9	11.3	13.3	16.9	9.0	9.0	10
$\rho_g/\rho_l \times 10^3$	45	9.5	22	5.8	1.3	25	10–50
$\mu_g/\mu_l \times 10^2$	4.9	0.1	2.7	2.2	1.8	1.8	3
$Re_l \times 10^{-5}$	6.3	12	5	3	0.9	0.4	5
$Re_g \times 10^{-5}$	2.1	3.3	6.5	3.6	0.14	4.1	4
$We_g \times 10^{-5}$	11.0	8.4	8.7	1.4	0.03	0.2	1–10

[a]Preburner. [b]Main combustion chamber.

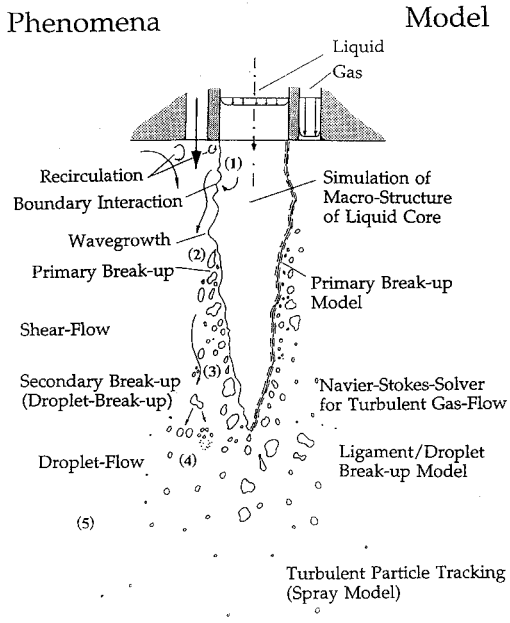

Fig. 1 Coaxial atomization model and phenomena.

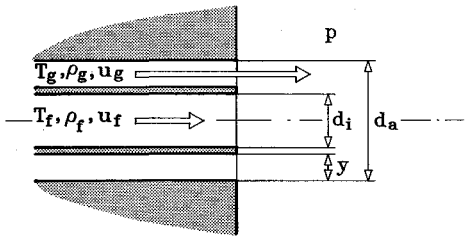

Fig. 2 Geometry of coaxial injector.

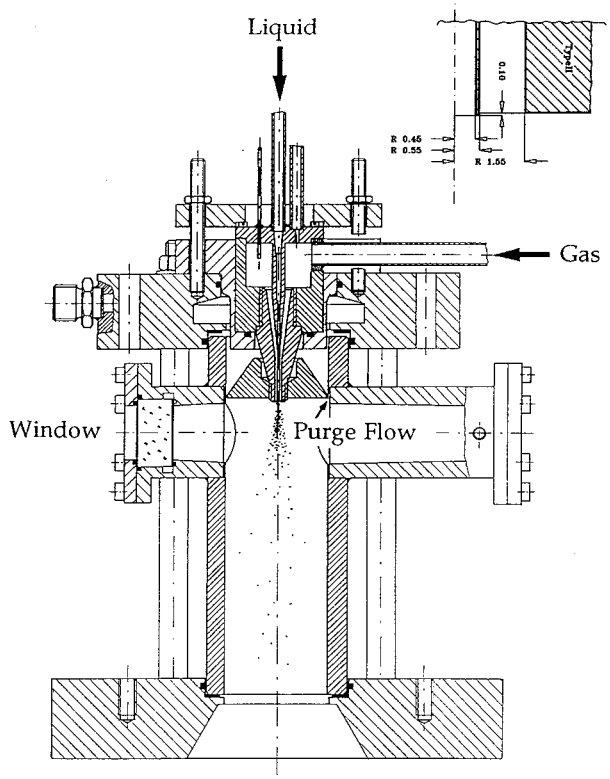

Fig. 3 Test chamber and injector tip detail.

compares the data of presently used engine injectors, summarized as "typical values," with model experiments performed in this study.

Model I was operated with the simulation fluids H_2O and air under ambient conditions. A large range of flow states was investigated, mainly by flow visualization studies, where a number of results are already published in Ref. 3.

Pressurized Test Chamber Experiments

Increased representativity of experiments could be achieved in a pressurized test chamber (Fig. 3). In particular, the liquid/gas density ratio ρ_g/ρ_l, and the Weber number We_g reach a better, although still unsatisfactory, representation in the latter case approximation to typical values. This is due to the high surface tension of water compared to LO_2. The influence of increased gas density to the atomization process is shown in Fig. 4. Increasing gas density magnifies the aerodynamic interaction, resulting in a faster and finer atomization. This is in agreement with theoretical predictions (see Theoretical Part). The effect of increased gas density with respect to atomization morphology appears similar to increased gas velocity, which suggests a gas momentum dependence ($\rho_g u_g^2$) of the process.

Time Transient Atomization Studies

The time transient behavior of the global atomization process is investigated with a laser light sheet setup in connection with a high-speed "streak" camera (Cordin 351). With the laser light sheet method, in contrast to the shadowgraph method, it is possible to obtain photographs of the liquid core through the thick spray. The light source, a copper vapor laser (Oxford Lasers Ltd.[9]) gives ~20-ns pulses with a repetition rate of up to 30 kHz. With this equipment it was possible to get a series of ~80 photographs that could be used to create animated video sequences of the atomization process. These sequences show all the relevant stages of atomization as, e.g., the growth

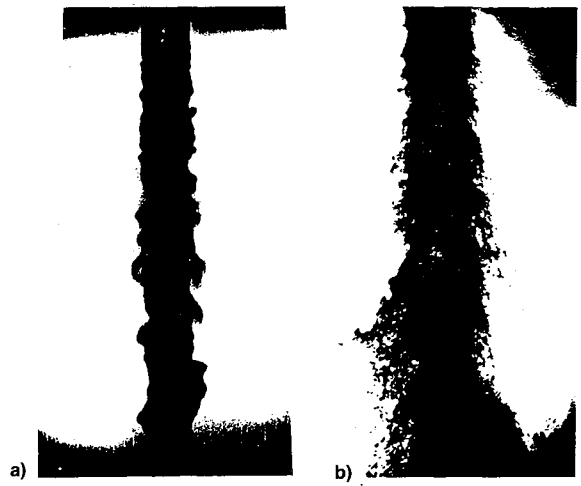

Fig. 4 Test chamber results water/air, u_l = 10 m/s, u_g = 100 m/s, d_{jet} = 2 mm, chamber pressure: a) 1 and b) 20 bar.

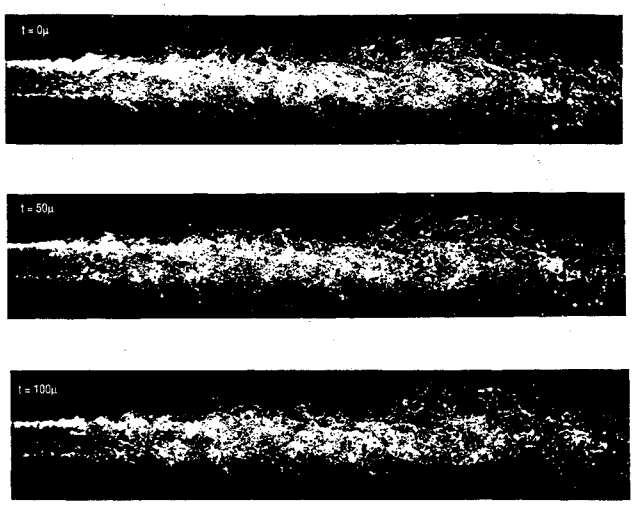

Fig. 5 Sequence of coaxial atomized jet. Laser light sheet, Δt = 50 μs, u_{jet} = 22 m/s, u_{gas} = 15 m/s.

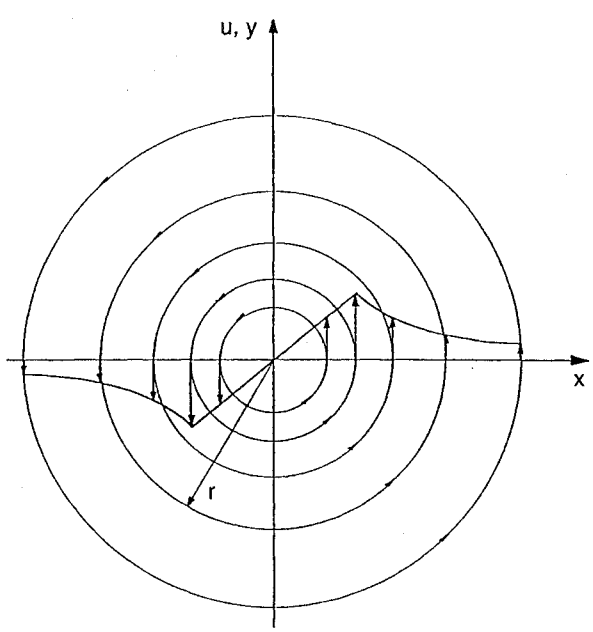

Fig. 6 Velocity field of symmetrical model eddy.

of surface waves and the stripping off and acceleration of the droplets. An exemplary sequence is presented in Fig. 5. These flow visualization studies are essential for the understanding of the flow phenomena, which is the basis for the development of atomization models.

Theoretical Part

Liquid Turbulence

As the experiments suggest, the turbulence inside the liquid jet is responsible for the initiation of jet breakup. Measure-

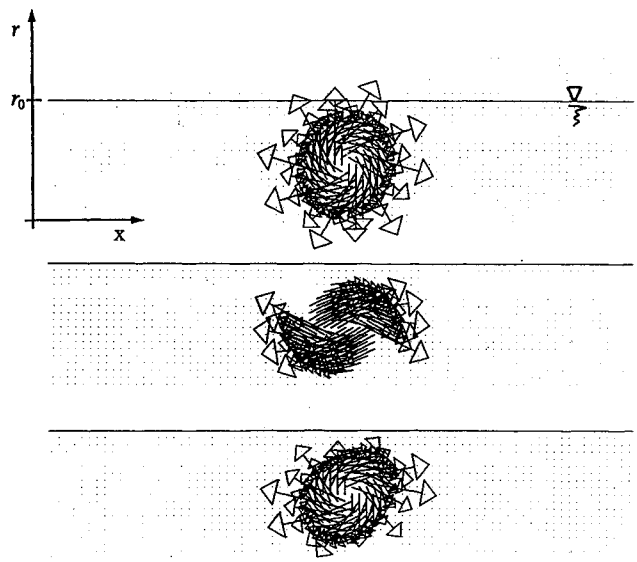

Fig. 7 Different types of model eddies.

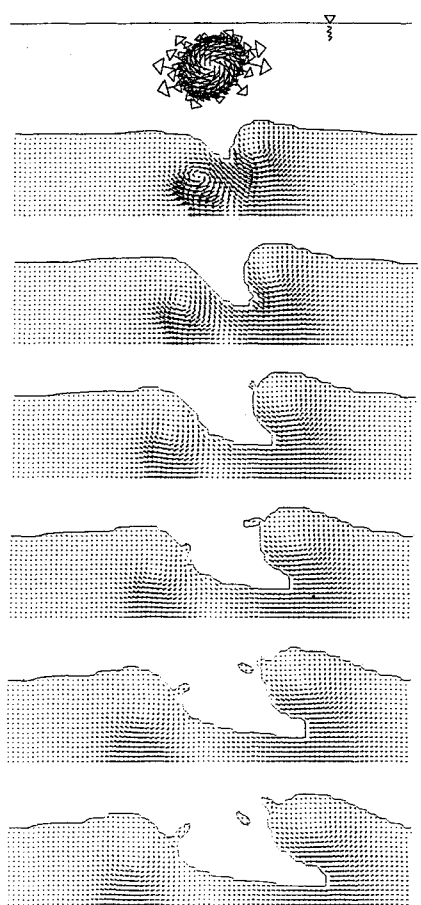

Fig. 8 Model eddy in interaction with liquid surface, u_{max} = 4.7 m/s, Δt = 200 μs.

ments or flow visualization inside the liquid jet and core that resolve internal flow phenomena are not possible at present. Thus, numerical simulations of liquid jet evolution including surface tension effects have been performed.[7,8]

The flowfield at the nozzle exit is that of a turbulent pipe flow. Measurements from Laufer[10] and Lawn,[11] and the results from large-eddy simulations[12] indicate that the turbulent structures with the highest energy level have a size of approximately 10–30% of the tube diameter. These eddies are expected to contribute primarily to liquid surface disturbances.

The statistical process of turbulence is approximated using model structures or eddies whose time-transient behavior in conjunction with the liquid surface is calculated. Different types of two-dimensional eddy models were used, namely, symmetrical and radially and ellipsoidally deformed Rankine eddies to consider the sensitivity of calculation to anisotropy of pipe turbulence. The velocity field of the Rankine eddy (see Fig. 6) is a combination of the kinematics of a solid body rotation with that of a potential vortex, and is characterized by its dimension and maximum velocity u_{max}. The kinds of the model eddies used in the calculations is shown in Fig. 7.

In the following studies the influence of ambient gas is neglected. The surface-tracking method used is adopted from the volume-fluid method (VOF) developed by Hirt et al.[13] A result of the computations shows that the influence of eddy shape is small compared to the influence of eddy energy. Figures 8 and 9 compare a weakly and a highly turbulent jet segment, respectively. The interaction of a low-energy symmetric eddy makes it obvious that tube turbulence has a deforming influence on the liquid surface. The simulations also indicate that higher turbulence levels lead to a disruption of the jet as an effect of liquid velocity fluctuations alone, in the absence of swirl or influence of ambient gas (see Fig. 9). For a free turbulent jet, emerging from a straight tube, a qualitative agreement between experiment and simulation was found. This comparison is shown in Fig. 10.

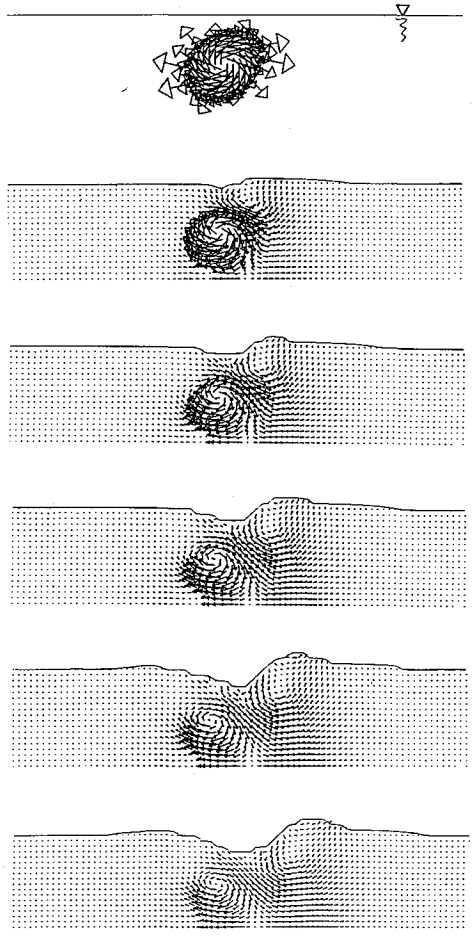

Fig. 9 Model eddy in interaction with liquid surface, u_{max} = 18.7 m/s, Δt = 200 μs.

Gas-Liquid Interaction

Generally, the influence of a surrounding fast gas flow leads to an increase of surface wave growth and to macroscopic instabilities of the liquid jet, and finally, to a faster atomization of the liquid. Figure 11 shows the influence of ambient gas to surface waves as a comparison of a liquid jet with and without coaxial airflow. The behavior of symmetric, small-scaled (i.e., small compared to the jet radius) surface waves is investigated applying a first-order linear stability analysis that ultimately leads to a dispersion Eq. (5), which describes the wave growth as a function of wavelength. A typical result is shown in Fig. 12, where the positive or negative value of wave growth indicates unstable or stable regions, respectively. The experimentally observed tendency of increasing gas density to result in faster and finer atomization is in consistent

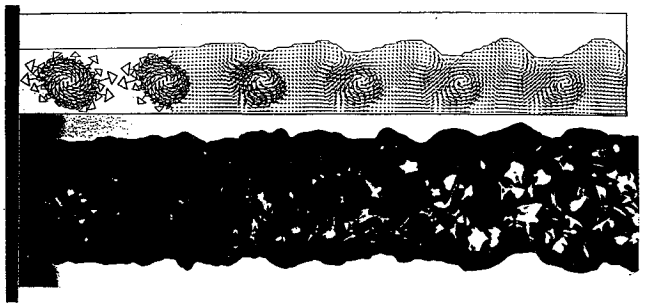

Fig. 10 Turbulent free liquid jet, u_{jet} = 13 m/s, Re = 1.3 × 10^4, σ = 0.07 N/m, simulation (top) and experiment (bottom).

Fig. 11 Segment of a free liquid jet, Re_l = 10^4: a) without coaxial gas and b) with coaxial gas: u_{rel} = 100 m/s.

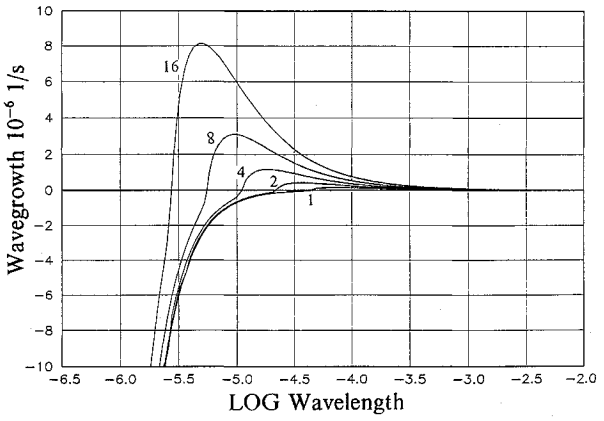

Fig. 12 Amplitude growth of axisymmetric instabilities vs wavelength, reference state is water/air under ambient conditions, $u_r = u_g - u_l$ = 100 m/s, parameter is the gas density.

agreement with the computation outcome. Results in the form of further parametric studies are published in Ref. 3.

In continuing these studies, the azimuthal disturbance of jet surface is included, which leads to the following form of surface displacement:

$$\eta(z, \theta, t) = \Re[\eta_0 \exp(ikx + im\theta + \omega t)] \qquad (4)$$

where η_0 is an initial disturbance level, $k = 2\pi/\lambda$ the wave number, and ω the complex wave growth rate (see Fig. 13). This surface displacement is imposed on the initial steady motion of a round liquid jet. The response of the liquid gas boundary is described by the linearized Navier-Stokes equations with the assumption of incompressible flow. The gas boundary is approximated assuming a $\frac{1}{7}$-power law for the velocity distribution between liquid surface and free gas flow (see Fig. 14). This model boundary assumption enters into the dispersion Eq. (5) as the damping factor ξ.

The behavior of the $m = 1$ mode, which in the longwave range exhibits a macroscopic serpentine jet oscillation, is plotted against the wave length and varies with the gas density (see Fig. 15). The reference state is a water/air system under ambient conditions with a relative velocity $u_r = u_g - u_f = 100$ m/s. Apparently, the most unstable wavelength is independent of the density ratio $\lambda_{max} \sim 4 \times r_0$. This is in agreement with the experimental observation that $m = 1$ oscillations appear only (if at all) in a narrow band around λ_{max} (see Fig. 16).

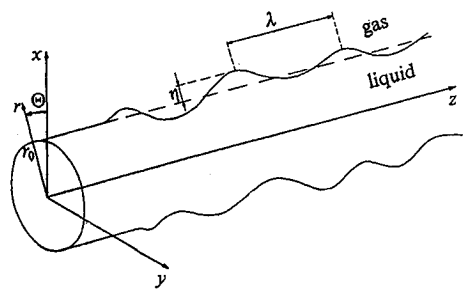

Fig. 13 Flow configuration, parameters of the jet deformation.

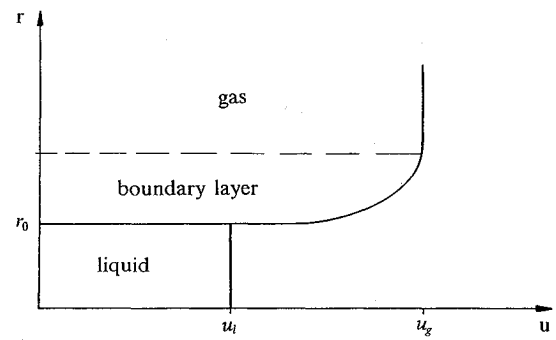

Fig. 14 Liquid and gas velocity distribution, $\frac{1}{7}$-power boundary-layer assumption.

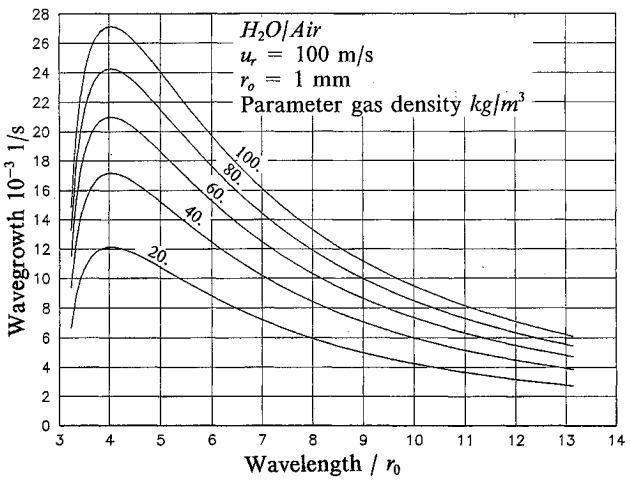

Fig. 15 Amplitude growth of the nonaxisymmetric $m = 1$ mode of a liquid jet vs wavelength. Water/air, $u_r = u_g - u_f = 100$ m/s, parameter is the gas density.

For higher modes of instability ($m \to \infty$), only the small wavelength range becomes significant. This tendency is shown in Fig. 17 for two extreme reference states, namely, the Space Shuttle Main Engine preburner (SSME preburner) and H_2O/air under ambient conditions (see Table 1), where the bifurcation points (the boundaries between stable and unstable oscillation) are plotted against the mode of oscillation. The theoretical and experimental observation is that only small wavelengths grow, except the $m = 1$ mode, which seems to be superimposed onto the small-scale disturbances.

Primary Breakup Model

The requirements on a ("sub grid scale") primary breakup model is to compute the frequency, the mass or diameter, and the location of the detached droplet. A further result is the shape of the liquid core. The proposed model leads to analytic equations that are solved along the jet surface, taking into account the change of mean flow quantities of gas and liquid. The calculation steps of the primary atomization model may be summarized as follows (for more modeling details see Ref. 8): 1) assessment of turbulent length scale appearing at the jet surface as a result of an (presently) empirical (or analytical) equation of liquid jet turbulence, 2) calculation of aerodynamic amplification of surface disturbances, and 3) calculation of the mass stripped off the jet.

The calculation of the wave growth ω as a function of wave length λ is done solving the linearized Navier-Stokes equations, including surface tension and assuming a sinusoidal wave shape. This leads to the following complex nonlinear equation for the wave growth ω:

$$\omega^2 + 2\nu_f k^2 \omega \left[\frac{I_1'(kr_0)}{I_0(kr_0)} - \frac{2kl}{k^2 + l^2}\frac{I_1(kr_0)}{I_0(kr_0)}\frac{I_1'(lr_0)}{I_1(lr_0)}\right]$$
$$= \frac{\sigma_f k}{\rho_f r_0^2}[1 - (kr_0)^2]\frac{l^2 - k^2}{l^2 + k^2}\frac{I_1(kr_0)}{I_0(kr_0)}$$
$$+ \xi\frac{\rho_g}{\rho_f}\left(U - \frac{i\omega}{k}\right)^2 k^2 \frac{l^2 - k^2}{l^2 + k^2}\frac{I_1(kr_0)}{I_0(kr_0)}\frac{K_0(kr_0)}{K_1(kr_0)} \qquad (5)$$

where I_m and K_m are modified Bessel functions of the first and second kind of mth order, respectively, and $l^2 = k^2 + \omega/\nu_l$, where ν_l is the liquid kinematic viscosity. It could be shown that this equation describes in representative cases also the behavior of nonlinear (nonsinusoidal) waves.[8]

A breakup criterion was used that proceeds from the assumption that detached droplets have diameters with a size in the order of the surface disturbance length scales. Breakup is predicted if the wave exceeds a critical scale, assumed to be reached if the wave amplitude exceeds the wave length that results in a droplet diameter $d \sim \lambda/\sqrt[3]{2}$. The results of the primary atomization model serve as an input for the following spray calculation. In the case that the stripped droplet exceeds a critical Weber number, secondary breakup occurs, which is another droplet/gas interaction phenomenon, as described e.g., in Mayer et al.[6]

Global Spray Simulation

The coupling of the models for primary and secondary breakup, and the turbulent droplet dynamics together with the gas and liquid (in-)flow conditions represent the basic structure of the global coaxial atomization and mixing model

Fig. 16 Nonaxisymmetric oscillations of a liquid jet water/air: a) d_{jet} = 1 mm, u_f = 10 m/s, u_g = 50 m/s, p_g = 10 bar and b) d_{jet} = 2 mm, u_f = 3 m/s, u_g = 150 m/s, p_g = 1 bar.

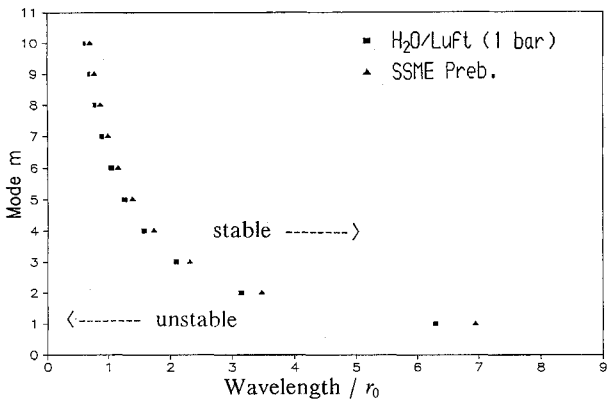

Fig. 17 Bifurcation points of mode *m*, reference states: SSME preburner and water/air under ambient conditions.

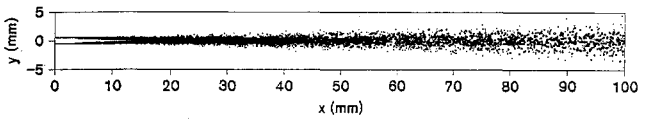

Fig. 18 Global spray simulation; water/air, theoretical laser light sheet thickness is 0.1 mm, d_{jet} = 2 mm, $u_{l,in}$ = 20 m/s, $u_{g,in}$ = 150 m/s.

(see sketch of model Fig. 1). A typical result of a simulation with that model is presented in Fig. 18 that shows the simulated atomization and mixing of a water jet in air. The atomization results in a broad spectrum of droplet diameters. The spray angle for the smaller and larger droplets is mainly the result of gas turbulence and Saffman-lift,[14] respectively. This result could be found out from parameter studies published in Ref. 6.

Droplet trajectories are described in the stochastic separated flow formulation in which secondary broke-up droplets were tracked as droplet parcels. The momentum exchange between droplets and gas is considered in the particle-source-in-cell method proposed by Crowe et al.[15]

The global atomization model is a tool with which to study influential parameters and to improve detailed submodels under realistic conditions, e.g., by the implementation of that model into a combustion chamber flow calculation.

Concluding Remarks

The crux of experimental work performed was the time transient flow visualization of the coaxial atomization. With the laser light sheet setup it was possible to gain insight into the atomization process along the liquid core inside the thick spray by visualizing breakup details in different parameter regions.

The study of atomization under elevated pressures up to 20 bar shows finer and faster atomization in comparison to 1-bar experiments. This is in agreement with theoretical assessments.

As an important result of experiments and theory, proof has been obtained of the impact of fluid jet internal motions on surface irritation. On the one hand, high-speed films were evaluated to correlate injection Reynolds number to surface evolution, and on the other hand, direct numerical simulations were applied, with the possibility to gain insight into the liquid core, using model eddies with the result of qualitative agreement between simulation and experiment. Simulations including gas interaction indicate that the wavelength and initial state of the disturbance is mainly influenced by liquid turbulence, whereas the wavegrowth, -deformation and -detachment is to a large extent the result of aerodynamic forces.

The m = 1 nonaxisymmetric oscillation mode of the liquid jet seems to be superimposed onto small-scale jet disturbances. This leads to a three dimensionality of the coaxial atomization and mixing process.

The global atomization model provides results in terms of droplet spectra that show qualitative and quantitative compliance with experimental evidence, patternator, and phase Doppler particle analyzer measurements.

References

[1]Liang, P., Fisher, S., and Chang, Y., "Comprehensive Modeling of a Liquid Rocket Combustion Chamber," *Journal of Propulsion and Power*, Vol. 2, No. 2, 1986, pp. 97–104.

[2]Przekwas, A., Chuech, S., and Singhal, A., "Numerical Modeling for Primary Atomization of Liquid Jets," AIAA Paper 89-0163, Jan. 1989.

[3]Krülle, G., Mayer, W., and Schley, C.-A., "Recent Advances in H2/O2 High Pressure Coaxial Injector Performance Analysis," AIAA Paper 90-1959, July 1990.

[4]Faragó, Z., "Dimensional Analysis of Aerodynamical Atomization," *Sprays and Aerosols '91*, edited by W. Balachandran, ILASS-Europe and the Aerosol Society UK, Guildford, Univ. of Surrey, England, UK, 1991.

[5]Buschulte, W., "Liquid Atomization by Injector Nozzles, *Proceedings of the ISABE, 9th International Symposium on Air Breathing Engines* (Athens, Greece), 1989, pp. 977–986.

[6]Mayer, W., Labani, R., and Krülle, G., "Theoretical Investigations of Droplet Flow Under Typical Coaxial Flow Conditions of Cryogenic Rocket Engines," AIAA Paper 92-3121, July 1992.

[7]Mayer, W., "Zur koaxialen Flüssigkeitszerstäubung im Hinblick auf die Treibstoffaufbereitung in Raketentriebwerken; Coaxial Liquid Atomization and Mixing of Propellants in Rocket Engines," Ph.D. Dissertation, LSTM, Univ. Erlangen-Nürnberg, Germany; also DLR Research Rept., DLR-FB 93-09, Germany, 1993.

[8]Mayer, W., "Investigation and Modeling of Coaxial Atomization in Liquid Rocket Engines," DLR Rept., DLR IB 643-94-03, DLR, Hardthausen, Germany, 1994.

[9]Oxford Lasers, Ltd., Newtec Place, Magdalen Road, Oxford, England, UK, 1992.

[10]Laufer, J., "The Structure of Turbulence in Fully Developed Pipe Flow," National Bureau of Standards, Rept. 1174, United Kingdom, 1954.

[11]Lawn, C. J., "The Determination of the Rate of Dissipation in Turbulent Pipe Flow," *Journal of Fluid Mechanics*, Vol. 48, Pt. 3, 1971, pp. 477–505.

[12]Krülle, G., Mayer, W., Schley, C.-A., and Faragó, Z., "Status of Coaxial Injector Modelling and Experiments at DLR Lampoldshausen," 18th International Symposium on Space Technology and Science, Kagoshima, Japan, 1992.

[13]Hirt, C. W., and Nichols, B. D., "Volume-of-Fluid (VOF) Method for the Dynamics of Free Boundaries," *Journal of Computational Physics*, Vol. 39, 1981, pp. 201–225.

[14]Saffman, P. G., "The Lift on a Small Sphere in a Slow Shear Flow," *Journal of Fluid Mechanics*, Vol. 22, Pt. 2, 1965, pp. 385–400.

[15]Crowe, C. T., Sharma, M. P., and Stock, D. E., "The Particle-Source-In Cell (PSI-CELL) Model for Gas-Droplet Flows," *Journal of Fluids Engineering*, Vol. 99, No. 2, 1977, pp. 325–332.